Heliyon 10 (2024) e26122

Contents lists available at ScienceDirect

Heliyon

journal homepage: www.cell.com/heliyon

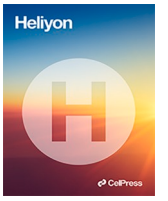

Research article

Prediction of tensile modulus based on parameters of crystalline structure in polyethylene terephthalate with cold crystallization ability

Ali Zarbali *, Ilies Djaffar, Alfréd Menyhárd

Laboratory of Plastics and Rubber Technology, Department of Physical Chemistry and Materials Science at Budapest University of Technology and Economics, H-1111 Budapest, Műegyetem rkp. 3., Hungary

A R T I C L E I N F O

Keywords:
Mechanical properties
Prediction model
poly(ethylene terephthalate)
Melting curve
Cold crystallization

A B S T R A C T

This work aims to adopt a simple modulus prediction method for the crystalline poly(ethylene-terephthalate) (PET), which has strong cold-crystallization ability. Based on a single melting curve generated by calorimetry, crystallinity and average melting temperature can easily be evaluated and consequently, tensile modulus can be predicted. Nonetheless, in the case of polymers with cold crystallization behavior, such as PET, the melting process is affected by cold crystallization, impeding the simple calculation of the aforementioned important parameters. In this paper, the techniques to eradicate cold crystallization during calorimetry are presented. Accordingly, the results of a tensile modulus prediction model are presented and discussed. The crystallization and melting characteristics of PET were measured by differential scanning calorimetry (DSC). The mechanical properties of the specimens were estimated by standardized tensile tests. The specimens, which were used for mechanical tests were fabricated using conventional injection molding. The samples were annealed at different temperatures in order to obtain different crystalline structures. The results clearly indicate that the prediction technique is capable to describe the tensile modulus of PET accurately in the case of very diverse crystalline structures.

1. Introduction

The improvement of mechanical properties of semicrystalline polymeric materials has been of crucial importance in the past decades, since the targeted modifications of the crystalline structure is accompanied by proportional changes in properties [1]. Over the last couple of decades, various studies have been conducted on the correlation between crystalline structure and mechanical properties of semicrystalline polymers [2–7]. Several micromechanical models have been developed to demonstrate and predict the mechanical behavior of semicrystalline polymers [6,8–10]. These micromechanics modeling methods were used to estimate the overall elastic, viscoelastic, and plastic mechanical properties of polymer materials [11–15]. Based on the results of such models, it has been observed that the presence of the crystalline lamellae enhances the mechanical properties. Besides, it is important to mention that Pukánszky et al. have shown that two key structural parameters that predominantly influence the modulus are crystallinity and lamellae thickness Pukánszky et al. [16]. Yet, the interplay between the crystalline phase and the amorphous phase and its influence on the overall

* Corresponding author.
E-mail address: ali.zarbali@edu.bme.hu (A. Zarbali).

https://doi.org/10.1016/j.heliyon.2024.e26122
Received 12 October 2023; Received in revised form 10 January 2024; Accepted 5 February 2024
Available online 13 February 2024

mechanical behavior of the polymers is still mechanically unquantified [17]. Up till now, there is no single model that is generally valid for polymers that describes the intricate relationship between the microstructure parameters and mechanical properties, due to factors like chemistry, crystallization kinetics, and type of crystallization [18]. Different models treat the molecular architecture distinctively, with specific assumptions. Among the notable prediction models, there is the modified Halpin-Tsai Model [19], which includes the volume fractions and modulus of both the crystallites and amorphous phase. The modified Guth-Gold model employs an empirical equation and handles the crystalline regions as reinforcing particles embedded within the amorphous matrix [20]. There are approaches that derives benefit of Voigt and Reuss models which are two complementary models where upper and lower limits of the composite modulus can be calculated [21,22]. The Rule of Mixtures is a simpler and more intuitive model that presumes a linear connection between a composite's modulus and the volume percentages of its component phases [23]. Mori-Tanaka model is an expansion of the Voigt model, which considers the impact of microstructural heterogeneity [24]. Even though the aforementioned models and techniques have been employed during several studies, their inaccuracies and limitations hinder their widespread application. Some of them are effective only for specific types of semicrystalline polymers or in the case of particular microstructural configurations. Although these models satisfy the theoretical predictions, their accuracy lacks experimental validation. Most of the models require complex and time-consuming calculations and constants which are not known for most of the polymers.

In this study, an empirical model is employed that is built on a logistic function correlating the tensile modulus with crystallinity and average melting temperature. To give more context, it should be mentioned that in the former versions of the model, lamella thickness was present in the equation [25], however since evaluation of lamella thickness is considerably challenging and time-consuming, it has been replaced by average melting temperature which is much easier to calculate. The average melting temperature, which is the weight average temperature of the melting peak is considered as a characterization of lamella thickness based on earlier findings where a directly proportional relationship between the two had been shown [26]. Our empirical approach itself is based on an earlier study as well, where Pukánszky et al. demonstrated the link between the stiffness of polypropylene with crystallization characteristics and showed that the key structural parameters of modulus are crystallinity and lamellar thickness [16,27]. The most significant advantages of our model are that all the necessary information for the prediction of modulus can be gathered from a simple calorimetric measurement and the equation is valid in the entire crystallinity range. Even though in our preceding works an exponential function had been used [25,26], later in the most recent study, it was concluded that a logistic function not only gives better estimations but also makes the prediction of moduli in higher crystallinity ranges more realistic and describes always the expected sigmoid type correlation [28].

$$E = E_a + \frac{E_c - E_a}{1 + \left(\left(\frac{1-X}{X} \right)^{\alpha} + \left(\frac{T_m^0 - T_{av}}{T_m^0} \right)^{\beta} \right)^{\gamma}} \tag{1}$$

where, E_a and E_c are the tensile moduli for completely amorphous and perfectly crystalline polymer, respectively. X is the crystallinity, T_{av} is the average melting temperature, T_m^0 is the equilibrium melting temperature, and α, β, γ are iterative empirical constants. The iterative constants have been generated during previous studies for iPP, PA6 and PLA [26,29].

PET has excellent physical and chemical properties, specifically, favorable mechanical performance and thermal resistance as well. These qualities make it to be one of the most demanded and broadly used semi-crystalline thermoplastic polyesters with applications in the fields of beverage bottles, packaging, textiles. There have been wide investigations on crystallization kinetics and the effect of crystallization on tensile properties of PET [30–33]. Yet, not many studies have been reported that examine the kinetics and mechanisms of cold crystallization and scarcely any study has been seen by the present authors that investigates the effect of cold crystallization kinetics on the prediction of mechanical properties. Therefore, considering all these, selecting PET as material for our modulus prediction study is not a coincidence. PET is one of the polymers which can undergo cold crystallization. Due to cold crystallization process, an exothermic peak appears often through the heating scan of a calorimetric measurement of PET. When the heating rate is slow, e.g. 10 K min^{-1}, there is sufficient time for the rearrangement of amorphous regions into a crystalline phase, which appears as a cold crystallization peak. According to the literature, crystallinity and molecular orientation influence the modulus of PET [18]. Due to the fact that it has a comparably slow crystallization rate and strain-sensitive characteristics, PET can be engineered to have a distinctive microstructure, which in turn leads to distinctive properties. Consequently, linking the mechanical behavior of PET with microstructure would be beneficial in the efficient designing of the manufacturing processes. Based on a study by Lyons, the theoretical modulus of PET was predicted at 146 GPa along the molecular axis, predicated on bond stretching [34]. However, the maximum value of modulus claimed for PET was an order of magnitude lower than the reported theoretical value, being 15.5 GPa for crystalline-oriented fibers [35].

The present study expands the application of our modulus prediction model to another semicrystalline polymer – poly(ethylene terephthalate) (PET). The main goal is to eliminate cold crystallization of PET at high heating rates to be able to successfully evaluate the average melting temperature and crystallinity based on the calorimetric curves and subsequently estimate the tensile modulus.

2. Materials and sample preparation

Two different commercial grades of PET were used during the modulus prediction study. One of them was NEOPET 80 copolyester grade supplied by Neo Group (intrinsic viscosity = 0.80 ± 0.02 dl/g, 100% PET composition), which was used for the development of the model, and the other was Arnite D00 301 PET granules by DSM Engineering Materials (intrinsic viscosity = 0.62 ± 0.01 dl/g), used for the verification.

Standard dumbbell shaped test specimens (ISO 527–1:2019) were produced by using DEMAG IntElect 560/330-100 type electronic injection molding machine. ISO 527 bars are preferred to repress the influence of the oriented skin, as within this type of specimens, mechanical characteristics are governed mostly by the core structure [28]. The temperature profile of injection molding process was 265–270–275– 280 °C and mold temperature was 80 °C. Injection pressure was set to 1800 bar with holding pressure of 400 bar. Holding and cooling times were both 25 s. Important to mention that the compounded materials were dried at 433 K for 4 h in an oven to eliminate the moisture content before injection molding. Once the specimens were fabricated they were set aside for a week in order to carefully eliminate post-crystallization effects since physical aging can alter the modulus during the first days following the processing [29]. Both types of the dumbbell shaped specimens were annealed at several temperatures to get different crystalline structures in a wide crystallinity range. The annealing temperatures were 353 K, 383 K, 443 K, 483 K, 503 K and 523 K. For the calorimetric tests, small samples were taken by cutting from the core part of the dumbbell specimens. Hermetically sealed aluminum crucibles were utilized as sample holder and the mass of the cut pieces were 3–5 mg. Nevertheless, in case of the fast scan DSC measurements the sample mass was kept between 0.5 and 1 mg.

3. Characterization and measurements

Tensile modulus evaluations were performed by employing Instron 5566 type tensile testing machine (Instron, Germany) based on ISO 527–1:2019 standards. Gauge length was 115 mm and crosshead speed 0.5 mm/min. Modulus values were measured below 0.3% deformation range.

Melting and crystallization characteristics were investigated by a PerkinElmer Diamond DSC apparatus. As purge gas, high-purity N_2 atmosphere (20 mL min^{-1}) was applied. The calorimeter was calibrated by high purity gallium, indium, and lead standard reference materials. DSC measurements were performed at different heating rates, starting from 10 K min^{-1} up to 500 K min^{-1}. In case of slow heating rate measurements, a single heating run from 303 to 583 K was carried out whereas in case of fast scanning rates, the samples were heated up to 673 K, considering the shift in melting peak.

There are two important values to be calculated in Eq. (1) for the prediction of modulus. These quantities can be evaluated solely based on a single calorimetric measurement. One of these parameters is crystallinity. Once the melting curve is generated, the corresponding crystallinity value can be obtained by the ratio of experimentally obtained enthalpy of fusion based on the melting curve to *equilibrium enthalpy of fusion*. In this work, the value for equilibrium enthalpy of fusion (ΔH_m^0) of PET was taken from literature, which was 140 J g^{-1} [36]. The other parameter to be evaluated from the melting curve is average melting temperature. The average melting temperature was obtained by following the same protocol as in earlier papers [26,28,29].

$$T_{av} = \frac{\int \dot{Q}\, T dT}{\int \dot{Q}\, dT} \tag{2}$$

Based on Eq. (2), the recorded heat flow curve was multiplied by temperature and the area under the resulting curve was calculated. Then the obtained value was divided by the area under the simple heat flow curve.

The stiffness of perfectly crystalline polymer was evaluated theoretically by measuring the propagation velocity of longitudinal sound waves in the specimens. The group velocity of longitudinal sound waves was measured in the annealed polymer samples using a VN Instrument SIA-7 NCA 1000-2E type ultrasonic equipment with air coupling transducers of 3.8 cm diameter and in 0.9 MHz–0.4 MHz broadband in transmission mode.

4. Results and discussion

As in earlier works, for the theoretical estimation of the modulus of perfect crystalline phase (E_c), the group velocity of longitudinal sound waves was calculated by applying a theoretical approach developed by van Krevelen [37]. For that, first, the velocity of the sound waves was computed based on the time of flight between first transmission and first reflection based on Eq. (3).

$$u_L = \frac{2d}{TOF} \tag{3}$$

Where u_L is the group velocity of the longitudinal sound wave, d is the thickness of the specimen and TOF is the time of flight between transmission and reflection.

The propagation rate of the waves depends on the crystallinity and experimental data was extrapolated to a 100% crystalline polymer as illustrated in the Fig. 1. To estimate E_c, the square of extrapolated velocity value was multiplied by the crystallite unit-cell density of PET (which is 1.455 g cm^{-3}) as given Eq. (4). The obtained E_c was 11.57 GPa. The tensile modulus of the amorphous PET was measured by a simple mechanical test on completely amorphous specimens, which was $E_a = 2.45$ GPa.

$$E_c = u_L^2 \rho_{cr} \tag{4}$$

Where u_L is the group velocity of the longitudinal sound wave, ρ_{cr} is the density of crystalline phase.

Throughout DSC experiments, we needed to evaluate only the first heating run, since the crystalline structure in that run is close to that of in the mechanical tests. During the heating scan of PET in calorimetric analysis a cold crystallization peak emerges, originating from the crystallization of the amorphous regions. The cold crystallization process hinders the precise assessment of the calorimetric

curves, as it is not possible to evaluate crystallinity from the enthalpy of fusion. If enthalpy of cold crystallization is subtracted from enthalpy of melting, crystallinity prior to cold crystallization can be obtained, as described in Eq. (5). However, this method is not safe since in this case average melting temperature value cannot be evaluated due to the fact that cold crystallization alters the crystalline structure of the specimen and consequently its melting characteristics too. Thus, in order to evade this issue, melting curves were generated by applying higher heating rates which lead to elimination of cold crystallization. Also, influence of increasing the heating rate on cold crystallization behavior was examined.

$$X = \frac{\Delta H_m - \Delta H_{cc}}{\Delta H_m^0} \tag{5}$$

Where ΔH_m and ΔH_{cc} corresponds to enthalpy of fusion and cold crystallization, respectively, and ΔH_m^0 is equilibrium enthalpy of fusion, value of which is taken from literature [36]. ($\Delta H_m^0 = 140\, J\, g^{-1}$).

Based on the demonstrated relationship between the heat of cold crystallization and different heating rates, it is obvious that enthalpy of cold crystallization follows a downward trend as the heating rate increases. Fig. 2 suggests that decrease in ΔH_{cc} continues till certain rate, which is 350 K min^{-1}, and above this value ΔH_{cc} remains constant at values close to zero. Basically, it can be deduced that at heating rates starting from 350 K min^{-1}, the cold crystallization seems to be eliminated.

As a solution to the previously mentioned issue, crystallinity and average melting temperature were calculated based on melting curves recorded at heating rate of 350 K min^{-1}, as there was no pronounced cold crystallization. Also, even though in this heating range, enthalpy of fusion values showed no considerable variation for the heating rate, it is still recommended to consider the possible effect of heating rate in case of using a new instrument. Because this value can be dependent on the implemented instrument [28].

Additionally, the influence of heating rate on average melting temperature was also analyzed. First, we eliminated the cold crystallization which impedes the evaluation of the curves, by annealing the specimens to study the effect of heating rate without cold crystallization process reliably. Needless to mention that throughout the annealing process samples undergo crystallization. In other words, later during the fast heating rate scans of DSC, no cold crystallization appears. Thus we annealed the samples at high temperatures like 503 K and 523 K and examined the impact of heating rate in a wide heating range. The dependence of average melting temperature on the selected heating rate is demonstrated in Fig. 3. According to the results, it is visible that there is a linear dependence; with an increment in heating rate, the average melting temperature increases as well.

It is also worth mentioning that in the case of samples that were heat treated at a higher temperature (at 523 K for example), the corresponding average melting temperature values were also higher at any heating rates respectively. The almost identical slopes indicate the fact that the correlation between the average melting temperature and the heating rate is affected only by the selected DSC instrument. Therefore, we have to highlight that this prediction method for samples with cold crystallization ability is reproducible for others only if they check once the dependency of T_{av} on the heating rate, by using their instrument.

If there is no heat treatment, meaning that the samples undergo cold crystallization during the first heating run, then evaluated average melting temperatures will not be fitted on a simple straight line like in the case of annealed samples shown in Fig. 3. The explanation is that at lower heating rates samples cold crystallize and the corresponding average melting temperatures appear to be higher than the ones with no pronounced cold crystallization (Fig. 4). The crystalline phase formed during the cold crystallization has larger structural stability than the crystalline phase formed during the dynamic cooling before the investigation of the sample. Therefore, the melting peak shifts to the higher temperature range.

Obviously, in this scenario, average melting temperatures are influenced by the selected heating rate in a linear fashion. Due to the fact that as we approach higher heating rates the cold crystallization ability is suppressed and this has effect on the average melting temperature. Therefore, the slopes of lines are not the same, unlike in the case of Fig. 3. Once we reach very high heating rates (in our

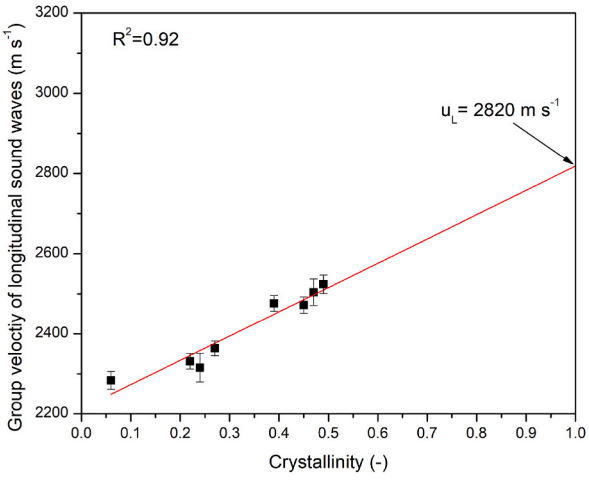

Fig. 1. Group velocity of longitudinal sound waves as a function of crystallinity.

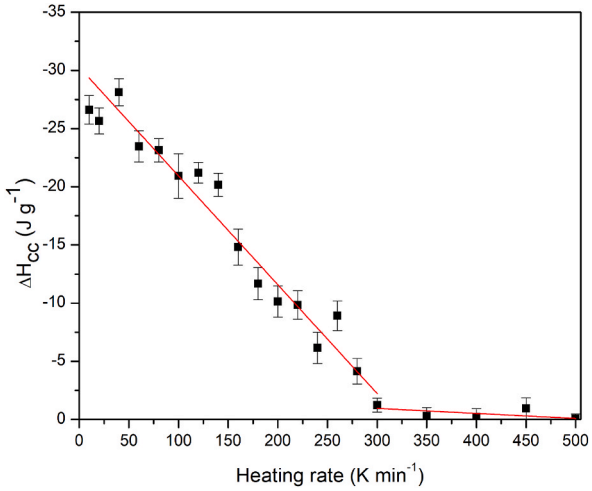

Fig. 2. ΔH_{cc} as a function of heating rate.

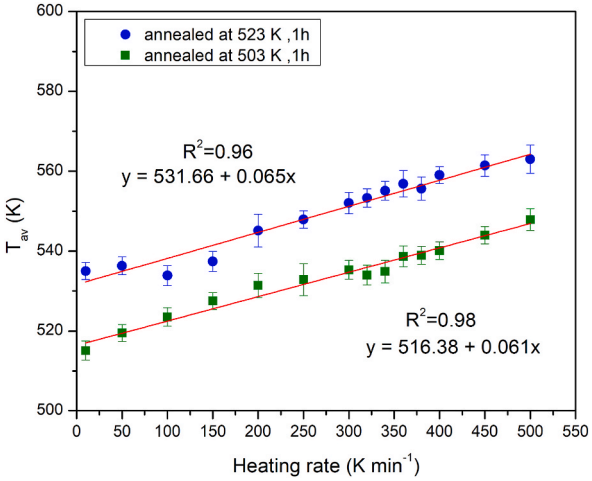

Fig. 3. Heating rate dependency of T_{av} for samples annealed at high temperatures.

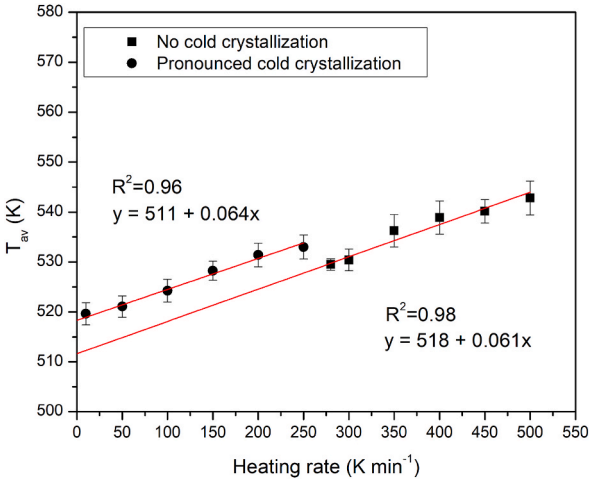

Fig. 4. Heating rate dependency of T_{av} for samples without heat treatment.

case 350 K min^{-1} and above), the cold crystallization disappears. The slope of the fitted lines is always around 0.061, thus we can clearly state that the shift of melting point as a function of heating rate depends only on the heating rate and on the instrument. It should be mentioned that the slope of the lines fitted to samples with cold crystallization is exactly the same compared to the high heating rate range and to the T_{av} values of the annealed samples.

In order to obtain the average melting temperature values for samples with pronounced cold crystallization ability, first it was needed to carry out the DSC measurements at 350 K min^{-1} and calculate the corresponding T_{av} values, and subsequently interpolate those T_{av} values to the standard 10 K min^{-1} of heating rate by using slope value of 0.061, which was evaluated in Figs. 3 and 4. Moreover, it should be emphasized that the slope is instrument dependent value and for different equipment it is required to determine it experimentally before the prediction procedure.

The average melting temperature values, which were obtained by interpolation to 10 K min^{-1} heating rate should be plotted as a function of crystallinity. The results are presented in Fig. 5. It is well discernible that the crystallinity is proportional to lamellar thickness and the strong correlation makes it possible to describe the T_{av} values by crystallinity. We have to point out that this correlation does not exist always. It exists here since all the points are recorded using the same PET polymer, in which only the annealing conditions were different. Earlier experiences clearly demonstrated that T_{av} (lamellar thickness) and crystallinity are two independent variables and they have to be determined always experimentally during the application of the prediction model. An exponential equation was applied for description of the T_{av} – X correlation:

$$T_{av} = T_{av,0} + Ae^{\frac{(x-x_0)}{t}} \tag{6}$$

The variables of A, x_0, and t are iterative parameters which have no physical meaning. It should be mentioned that T_{av} equals to the equilibrium melting temperature which is 568K according to literature [38] in a perfect crystal (at X = 1). After fitting the exponential function to the T_{av} – X data, the iterative parameters were found to be: A = 0.0922, x_0 = 0.59, t = 0.24. Fitting accuracy (coefficient of determination) is 0.99, which suggests a good correlation.

As demonstrated in Fig. 5, average melting temperature of annealed samples (no cold crystallization behavior) recorded at standard heating rate (10 K min^{-1}) were also added to the figure for comparison. These points are reasonably consistent with ones that were recorded at 350 K $min^{-1}$and interpolated to 10 K min^{-1}. It can be deduced that if the samples don't cold crystallize then it is possible to test them at 10 K min^{-1}. Otherwise it is necessary to run the DSC at high heating rates to eliminate the cold crystallization and allow the T_{av} evaluations.

The generated equation was plugged into the logistic model equation (Eq. 1) and thus T_{av} values were replaced, leaving the crystallinity as the only independent variable in the function. By doing so, it is possible to build a figure where tensile modulus is expressed as a function of crystallinity. Additionally, the iterative constants were estimated by fitting the model equation to tensile modulus – crystallinity data in the entire crystallinity range.

Observing the fitting results and considering the R^2 value in Fig. 6, it can be stated that the model equation demonstrates the modulus–crystallinity relationship effectively. Reading the figure, it is obvious that higher crystallinity leads to higher modulus. Even though the fitting precision is very good, there is an ambiguity regarding the high crystallinity region since there are no experimental points obtained. However, at the same time, from a practical point of view, the issue was inevitable, as reaching high crystallinity above 60 percent wasn't a possibility. Thus, using the correlation between the modulus of perfectly crystalline polymer, E_c and velocity of sound waves, u_L (see Eq. (4)), the modulus values at very high crystallinity region (97–100%) were theoretically obtained by extrapolating the experimental data.

After reaching a good fit of Eq. (1) on the experimental data, the iterative parameters (α, β, and γ) were estimated. In Table 1, the iterative constants and thermodynamic parameters are summarized including the present study of PET and a previous study where the

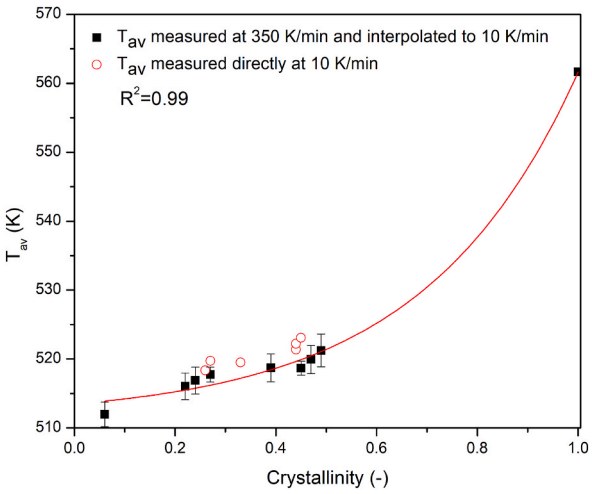

Fig. 5. Average melting temperature as a function of crystallinity.

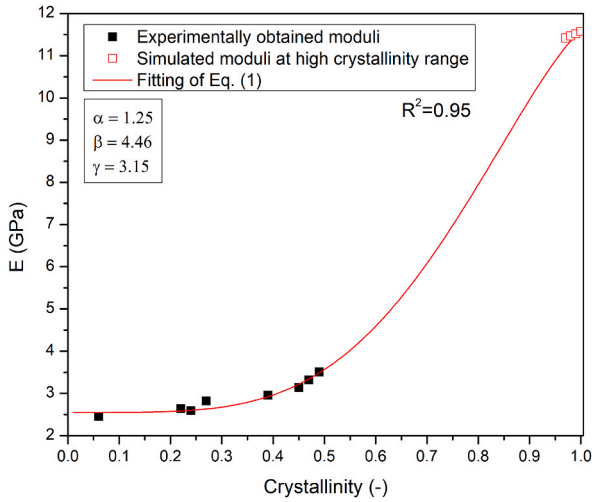

Fig. 6. Young's modulus as a function of crystallinity.

prediction model was applied to iPP [28]. We have to note that PP and PA6 do not have an affinity for cold crystallization, thus, fast scanning method is not necessary in their case and modulus prediction can be performed using the standard heating curve registered at 10 K min^{-1} of heating rate.

Samples were prepared and tested from another grade of PET (Arnite D00 301 PET granules by DSM Engineering Materials) to check the reliability of the evaluations and results. For the verification material too, the same procedure was followed: specimens were tested by calorimetry at heating rate of 350 K min^{-1} to eliminate the cold crystallization effect and average melting temperature and crystallinity were calculated from the curves, then T_{av} values were interpolated to 10 K min^{-1}. In the case of annealed samples where cold crystallization was no longer present, the melting curves were measured at 10 K min^{-1} of heating rate to test the reliability of our prediction method. T_{av} and crystallinity values were evaluated as it was described earlier and the modulus values were calculated using the model equation (Eq. 1). Also the modulus values were experimentally determined by tensile testing machine for further comparison with the predicted values. The correlation between the predicted and calculated values is presented in Fig. 7, including data from earlier studies on different polymers [26,28,29].

Based on the results shown in Fig. 7, it can be confidently stated that the results of the prediction model are reasonably good. The deviations are below 10 % which is in the acceptable region. The good agreement between experimentally determined and model-based evaluations proves the reliability of the technique. The model was already extended to polymers which tend to cold crystallize (the case of PLA) [29].

5. Conclusions

Estimation of the tensile modulus from a simple DSC run of PET with cold crystallization behavior was successfully achieved by applying the model equation. High heating rates (350 K min^{-1}) were applied and cold crystallization was eliminated. Average melting temperature and crystallinity values were obtained from the calorimetric curves. Subsequently, the evaluated average melting temperatures were interpolated to slow standard heating rate before calculating the moduli by model equation. Moreover, the modulus of completely crystalline PET was theoretically evaluated by using velocity of longitudinal sound waves in the material. The iterative constants required for model equation were estimated and then verified by using another grade of PET. Samples were annealed at several temperatures to attain different crystalline structures in a wide crystallinity range. Also, it was proved that the prediction method works well on PET samples which do not have cold crystallization (annealed or previously crystallized) without application of instrument dependent fast heating rates. Reasonably good agreement was found between experimental and predicted modulus values. The results prove that the model can possibly be applied to polymers that undergo cold crystallization.

Data availability statement

The processed data required to reproduce these findings will be made available on request.

CRediT authorship contribution statement

Ali Zarbali: Writing – review & editing, Writing – original draft, Visualization, Validation, Investigation, Conceptualization. **Ilies Djaffar:** Data curation. **Alfréd Menyhárd:** Writing – review & editing, Visualization, Supervision, Methodology, Conceptualization.

Table 1
Evaluated constants for different polymers, which are required to estimate modulus by Eq (1).

Polymer	T_m^0 (K)	ΔH_m^0 (J g^{-1})	E_a (GPa)	E_c (GPa)	α	β	γ
PET	583	140	2.45	11.57	1.25	4.46	3.15
iPP	481	148	0.01	6.6	0.33	0.35	4.80

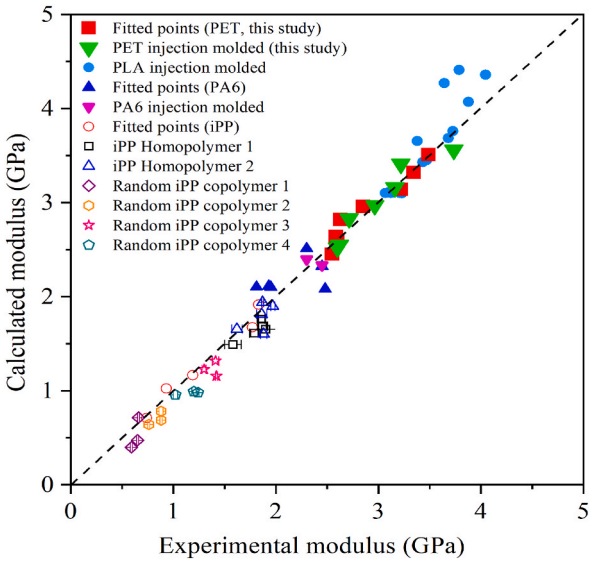

Fig. 7. Comparison of predicted and experimentally measured modulus.

Declaration of competing interest

The authors declare that they have no known competing financial interests or personal relationships that could have appeared to influence the work reported in this paper.

Acknowledgements

The research reported in this paper is part of project no. BME-NVA-02, implemented with the support provided by the Ministry of Innovation and Technology of Hungary from the National Research, Development and Innovation Fund, financed under the TKP2021 funding scheme.

Appendix A. Supplementary data

Supplementary data to this article can be found online at https://doi.org/10.1016/j.heliyon.2024.e26122.

References

[1] E.P. Moore, Polypropylene Handbook: Polymerization, Characterization, Properties, Processing Applications, Hanser/Gardner Publications, Cincinnati OH, 1996.
[2] B.A.G. Schrauwen, L.C.A.V. Breemen, A.B. Spoelstra, L.E. Govaert, G.W.M. Peters, H.E.H. Meijer, Structure, deformation, and failure of flow-oriented semicrystalline polymers, Macromolecules 37 (2004) 8618–8633, https://doi.org/10.1021/ma048884k.
[3] A. Galeski, Strength and toughness of crystalline polymer systems, Prog. Polym. Sci. 28 (2003) 1643–1699, https://doi.org/10.1016/j.progpolymsci.2003.09.003.
[4] A. Peterlin, Structural model of mechanical properties and failure of crystalline polymer solids with fibrous structure, Int. J. Fract. 11 (1975) 761–780, https://doi.org/10.1007/BF00012895.
[5] F. Bédoui, J. Diani, G. Régnier, Relationship between microstructure and elastic properties of semi-crystalline polymers, Mater. Res. Soc. Symp. Proc. 882 (2005) 110–115.
[6] V.A. Sedighiamiri, T.B. Erp, van, G.W.M. Peters, L.E. Govaert, J.A.W. Dommelen, Micromechanical modeling of the elastic properties of semicrystalline polymers: a Three-phase approach, J. Polym. Sci., Part B: Polym. Phys. 48 (2010) 2173–2184, https://doi.org/10.1002/polb.
[7] J. Karger-Kocsis, T. Bárány, Polypropylene Handbook: Morphology, Blends and Composites (2019), https://doi.org/10.1007/978-3-030-12903-3.

[8] D.R. Breese, G. Beaucage, A review of modeling approaches for oriented semi-crystalline polymers, Curr. Opin. Solid State Mater. Sci. 8 (2004) 439–448, https://doi.org/10.1016/j.cossms.2005.08.001.

[9] T.D. Horn, D. Heidrich, H. Wulf, M. Gehde, J. Ihlemann, Multiscale simulation of semi-crystalline polymers to predict mechanical properties, Polymers 13 (2021) 1–16, https://doi.org/10.3390/polym13193233.

[10] O. Gueguen, S. Ahzi, S. Belouettar, A. Makradi, Comparison of micromechanical models for the prediction of the effective elastic properties of semicrystalline polymers: application to polyethylene, Polym. Sci. 50 (2008) 523–532, https://doi.org/10.1134/S0965545X08050064.

[11] X. Guan, R. Pitchumani, A micromechanical model for the elastic properties of semicrystalline thermoplastic polymers, Polym. Eng. Sci. 44 (2004) 433–451, https://doi.org/10.1002/pen.20039.

[12] J. Diani, F. Bédoui, G. Régnier, On the relevance of the micromechanics approach for predicting the linear viscoelastic behavior of semi-crystalline poly (ethylene)terephtalates (PET), Mater. Sci. Eng. 475 (2008) 229–234, https://doi.org/10.1016/j.msea.2007.05.002.

[13] S. Nikolov, I. Doghri, O. Pierard, L. Zealouk, A. Goldberg, Multi-scale constitutive modeling of the small deformations of semi-crystalline polymers, J. Mech. Phys. Solid. 50 (2002) 2275–2302, https://doi.org/10.1016/S0022-5096(02)00036-4.

[14] J.A.W. Van Dommelen, D.M. Parks, M.C. Boyce, W.A.M. Brekelmans, F.P.T. Baaijens, Micromechanical modeling of the elasto-viscoplastic behavior of semi-crystalline polymers, J. Mech. Phys. Solid. 51 (2003) 519–541, https://doi.org/10.1016/S0022-5096(02)00063-7.

[15] S. Ahzi, A. Makradi, R.V. Gregory, D.D. Edie, Modeling of deformation behavior and strain-induced crystallization in poly(ethylene terephthalate) above the glass transition temperature, Mech. Mater. 35 (2003) 1139–1148, https://doi.org/10.1016/S0167-6636(03)00004-8.

[16] B. Pukánszky, I. Mudra, P. Staniek, Relation of crystalline structure and mechanical properties of Nucleated polypropylene, J. Vinyl Addit. Technol. 3 (1997) 53–57, https://doi.org/10.1002/vnl.10165.

[17] P.-E.M. Thanh, L. Nguyen, Fahmi B?edoui, mechanical investigation of Confined amorphous phase in semicrystalline polymers: case of PET and PLA, Society (2006) 1–10, https://doi.org/10.1002/pen.

[18] S. Bandla, M. Allahkarami, J.C. Hanan, Thermal crystallinity and mechanical behavior of polyethylene terephthalate, Conf. Proc. Soc. Exp. Mech. Ser. 2 (2015) 141–146, https://doi.org/10.1007/978-3-319-06980-7_17.

[19] J.C. Halpin, J.L. Kardos, The Halpin-Tsai equations: a review, Polym. Eng. Sci. 16 (1976) 344–352, https://doi.org/10.1002/pen.760160512.

[20] Y. Fukahori, A.A. Hon, V. Jha, J.J.C. Busfield, Modified Guth-Gold equation for carbon black-filled rubbers, Rubber Chem. Technol. 86 (2013) 218–232, https://doi.org/10.5254/rct.13.87995.

[21] R.H. Boyd, W. Bin Liau, Mechanical moduli of Spherulitic lamellar semicrystalline polymers, Macromolecules 19 (1986) 2246–2249, https://doi.org/10.1021/ma00162a022.

[22] R.H. Boyd, Prediction of polymer crystal structures and properties, Adv. Polym. Sci. 116 (1994), https://doi.org/10.1007/bfb0080195.

[23] P.T. Curtis, M.G. Bader, J.E. Bailey, The stiffness and strength of a polyamide thermoplastic reinforced with glass and carbon fibres, J. Mater. Sci. 13 (1978) 377–390, https://doi.org/10.1007/BF00647783.

[24] T. Mori, K. Tanaka, Average stress in matrix and average elastic energy of materials with misfitting inclusions, Acta Metall. 21 (1973) 571–574, https://doi.org/10.1016/0001-6160(73)90064-3.

[25] A. Menyhárd, P. Suba, Z. László, H.M. Fekete, O. Mester, Z. Horváth, G. Vörös, J. Varga, J. Móczó, Direct correlation between modulus and the crystalline structure in isotactic polypropylene, Express Polym. Lett. 9 (2015) 308–320, https://doi.org/10.3144/expresspolymlett.2015.28.

[26] J. Molnár, A. Jelinek, A. Maloveczky, J. Móczó, A. Menyhárd, Prediction of tensile modulus of semicrystalline polymers from a single melting curve recorded by calorimetry, J. Therm. Anal. Calorim. 134 (2018) 401–408, https://doi.org/10.1007/s10973-018-7487-1.

[27] Z. Horváth, A. Menyhárd, P. Doshev, M. Gahleitner, C. Tranninger, S. Kheirandish, J. Varga, B. Pukánszky, Effect of molecular architecture on the crystalline structure and stiffness of iPP homopolymers: modeling based on annealing experiments, J. Appl. Polym. Sci. 130 (2013) 3365–3373, https://doi.org/10.1002/app.39585.

[28] A. Zarbali, B. Pinke, A. Menyhárd, Robustness study of a tensile modulus prediction model for semicrystalline polymers, Period. Polytech. - Chem. Eng. 67 (2023) 232–241, https://doi.org/10.3311/PPch.20991.

[29] J. Molnár, A. Hertner-Horváth, A. Menyhárd, Prediction of tensile modulus from calorimetric melting curves of polylactic acid with pronounced cold crystallization ability, Polym. Test. 95 (2021), https://doi.org/10.1016/j.polymertesting.2021.107112.

[30] K. Zheng, X. Yao, L. Chen, X.Y. Tian, Isothermal crystallization kinetics and melting behavior of poly(ethylene terephthalate)/attapulgite nanocomposites studied by step-scan DSC, J. Macromol. Sci., Part B: Phys. 48 (2009) 318–328, https://doi.org/10.1080/00222340802679839.

[31] M. Zendehzaban, M. Shamsipur, Isothermal crystallization kinetics of poly(ethylene terephthalate)s of different molecular weights, J. Iran. Chem. Soc. 10 (2013) 77–84, https://doi.org/10.1007/s13738-012-0148-6.

[32] S. Yao, D. Hu, Z. Xi, T. Liu, Z. Xu, L. Zhao, Effect of crystallization on tensile mechanical properties of PET foam: Experiment and model prediction, Polym. Test. 90 (2020) 106649, https://doi.org/10.1016/j.polymertesting.2020.106649.

[33] X.F. Lu, J.N. Hay, Isothermal crystallization kinetics and melting behaviour of poly(ethylene terephthalate), Polymer (Guildf) 42 (2001) 9423–9431, https://doi.org/10.1016/S0032-3861(01)00502-X.

[34] W.J. Lyons, Theoretical values of the dynamic stretch moduli of fiber-forming polymers, J. Appl. Phys. 29 (1958) 1429–1433, https://doi.org/10.1063/1.1722962.

[35] J.W. Ballou, J.C. Smith, Dynamic measurements of polymer physical properties, J. Appl. Phys. 20 (1949) 493–502, https://doi.org/10.1063/1.1698416.

[36] A. Mehta, U. Gaur, B. Wunderlich, Equilibrium melting parameters of poly(ethylene terephthalate), J. Polym. Sci. Polym. Phys. Ed 16 (1978) 289–296, https://doi.org/10.1002/pol.1978.180160209.

[37] K. te N. D.W. van Krevelen, Properties of Polymers. Their Correlation with Chemical Structure; Their Numerical Estimation and Prediction from Additive Group Contributions, fourth ed., Amsterdam, 2009 https://doi.org/10.1016/0160-9327(92)90023-i.

[38] S. Fakirov, E.W. Fischert, R. Hoffmann, G.F. Schmidt, Structure and properties of poly(ethylene terephthalate) crystallized by annealing in the highly oriented state: 2.Melting behaviour and the mosaic block structure of the crystalline layers, Polymer 18 (1977).